



Review

The iron redox and hydrolysis chemistry of the ferritins

Fadi Bou-Abdallah *

Department of Chemistry, State University of New York at Potsdam, Potsdam, NY 13676, USA

ARTICLE INFO

Article history:

Received 6 January 2010

Received in revised form 23 March 2010

Accepted 26 March 2010

Available online 9 April 2010

Keywords:

Iron oxidation

Mineral core formation

Iron detoxification

Ferritin channel

Ferroxidase center

Di-iron peroxo complex

Di-iron oxo complex

Heteropolymer

H- and L-subunit

ABSTRACT

Background: Ferritins are ubiquitous and well-characterized iron storage and detoxification proteins. In bacteria and plants, ferritins are homopolymers composed of H-type subunits, while in vertebrates, they typically consist of 24 similar subunits of two types, H and L. The H-subunit is responsible for the rapid oxidation of Fe(II) to Fe(III) at a dinuclear center, whereas the L-subunit appears to help iron clearance from the ferroxidase center of the H-subunit and support iron nucleation and mineralization.

Scope of review: Despite their overall similar structures, ferritins from different origins markedly differ in their iron binding, oxidation, detoxification, and mineralization properties. This chapter provides a brief overview of the structure and function of ferritin, reviews our current knowledge of the process of iron uptake and mineral core formation, and highlights the similarities and differences of the iron oxidation and hydrolysis chemistry in a number of ferritins including those from archaea, bacteria, amphibians, and animals.

General Significance: Prokaryotic ferritins and ferritin-like proteins (Dps) appear to preferentially use H₂O₂ over O₂ as the iron oxidant during ferritin core formation. While the product of iron oxidation at the ferroxidase centers of these and other ferritins is labile and is retained inside the protein cavity, the iron complex in the di-iron cofactor proteins is stable and remains at the catalytic site. Differences in the identity and affinity of the ferroxidase center ligands to iron have been suggested to influence the distinct reaction pathways in ferritins and the di-iron cofactor enzymes.

Major conclusions: The ferritin 3-fold channels are shown to be flexible structures that allow the entry and exit of different ions and molecules through the protein shell. The H- and L-subunits are shown to have complementary roles in iron oxidation and mineralization, and hydrogen peroxide appears to be a by-product of oxygen reduction at the FC of most ferritins. The di-iron(III) complex at the FC of some ferritins acts as a stable cofactor during iron oxidation rather than a catalytic center where Fe(II) is oxidized at the FC followed by its translocation to the protein cavity.

© 2010 Elsevier B.V. All rights reserved.

1. Introduction

Iron is the most abundant transition metal on Earth and an essential element for many forms of life. It is found in the active sites of many enzymes and oxygen carrier proteins and is an important component of many cellular processes including respiration, electron transfer reactions, energy metabolism, DNA synthesis, and gene regulation. At physiological conditions, free iron exists primarily in one of two oxidation states, the relatively soluble ferrous (Fe²⁺) state and the very insoluble ferric (Fe³⁺) state with the solubility of the two ions being $\sim 10^{-1}$ and 10^{-18} M, respectively. The physiological ferric ion concentration is far too low to

support the growth of aerobic microorganisms that have developed various strategies to overcome this limitation.

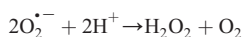
Moreover, the large variability in redox potential contributes significantly to the role of iron as an essential biological metal. The biological use of iron is thus limited by its low solubility and its propensity to participate in harmful free radical reactions. Consequently, living organisms were compelled to adopt efficient iron transport and storage mechanisms to obtain and safely balance the deleterious and beneficial effects of iron. For example, in bacteria and fungi, iron is mainly acquired by small organic molecules called “siderophores” that have a very high affinity for Fe(III) [1–3]. In plants, at least two strategies to acquire iron from the soil have evolved based on either reducing (i.e., ferric–chelate reductase) or chelating (i.e., siderophores) iron [4]. In animals, iron is mainly acquired from food with good to limited bioavailability depending on the source (i.e., iron is readily absorbed from red meat but has limited bioavailability in plants because of the presence of phosphates, phytates, and polyphenols that inhibit absorption by formation of insoluble complexes) and is transported and stored by a number of key proteins via a complex but fairly well-understood mechanism [5].

Abbreviations: Dps, DNA binding proteins from starved cell; HuHF and HuLF, human H-chain and L-chain ferritins; MtF, human mitochondrial ferritin; HoSF, horse spleen ferritin; BfMF, bullfrog M-chain ferritin; EcBFR and EcFtnA, heme- and nonheme-containing *Escherichia coli* ferritins; AvBF and DdBF, *Azotobacter vinelandii* and *Desulfovibrio desulfuricans* bacterioferritins; PfFtn and AfFtn, *Pyrococcus furiosus* and *Archaeoglobus fulgidus* archaeal ferritins; ITC, isothermal titration calorimetry; EXAFS, extended X-ray absorption fine structure; EPR, electron paramagnetic resonance spectroscopy; FC, ferroxidase center

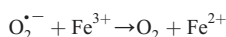
* Tel.: +1 315 267 2268; fax: +1 315 267 3170.

E-mail address: bouabdf@potsdam.edu.

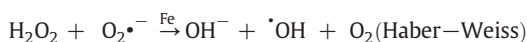
The wide range of the $\text{Fe}^{2+}/\text{Fe}^{3+}$ redox potential (from approximately -500 to $+600$ mV depending on the iron ligands and environment) and the facile ability of iron to gain and lose electrons allows it to participate in a wide variety of oxidation–reduction reactions [6] but at the same time underlies its toxicity. The one-electron reduction of dioxygen by Fe^{2+} results in the formation of superoxide radical $\text{O}_2^{\bullet-}$, which can accept another electron and two protons to produce hydrogen peroxide, H_2O_2 . Superoxide and hydrogen peroxide are the by-products of incomplete O_2 reduction, and their balance is regulated by the enzyme superoxide dismutase:



On the other hand, ferrous ions can react with hydrogen peroxide to generate the very reactive and damaging hydroxyl radical species (OH^\bullet) via Fenton reaction while superoxide radical ($\text{O}_2^{\bullet-}$) can reduce ferric iron to ferrous ions [7]:



The sum of these two reactions produces hydroxyl anion, hydroxyl radical and O_2 and is known as the Haber–Weiss reaction that only manifests in the presence of catalytic amounts of a redox metal such as iron:



One of the means to protect cells from the potentially toxic effects of free iron and radical chemistry is ferritin, a ubiquitous iron storage and detoxification protein [1,8–11]. Ferritins are a family of natural, highly conserved supramolecular nanostructures designed to sequester thousands of iron atoms in a mineralized and biologically available form for later use in heme and nonheme iron proteins and in biochemical reactions. The increased sensitivity to oxidative stress and the lethal effect on embryonic growth following deletion of the ferritin genes emphasize the importance of these proteins in early life development [12–16]. Another important property of ferritin and ferritin-like protein (also called Dps, DNA binding proteins from starved cell) is the protection of DNA from oxidative damage and organism nutritional deprivation and stress [17–21]. In this chapter, we will discuss our current knowledge of the process of iron uptake and accumulation in ferritin and review the chemistry of iron oxidation and deposition in a number of archaeal, bacterial, amphibian, and animal ferritins from a mechanistic and stoichiometric standpoint. Plant ferritins and the mechanism of iron release and the movement of iron and other ions through the ferritin shell are the subjects of separate chapters in this special issue and will not be discussed here.

2. Ferritin structural overview

2.1. Ferritins in mammals

Ferritins are composed of a protein shell surrounding a cavity where up to 4500 iron atoms can be accommodated as a macroinorganic iron complex. They have a unique molecular architecture typically composed of 24 structurally similar or identical subunits. Their main function is to detoxify and store cellular iron by coupling iron and oxygen (or hydrogen peroxide) to form a stable but biologically available ferric oxide mineral at nonreactive sites inside the ferritin cavity.

Extensive and important helix–helix interactions occur between ferritin subunits and loops resulting in unusually high protein stability (i.e., up to 80°C and to 6 M guanidine at neutral pH). Despite this web of

inter- and intrasubunits interactions, the protein maintains a flexible and dynamic structure that controls the flow of iron, oxidants, reductants, chelators, and small ligands and molecules in and out of its shell [22]. Unlike bacterial, fish, and amphibian ferritins, mammalian ferritins (with the exception of mitochondrial and serum ferritin) consist of two functionally and genetically distinct subunit types, H (heavy, $\sim 21,000$ kDa) and L (light, $\sim 19,000$ kDa) subunits. These two subunits coassemble in various ratios with a tissue-specific distribution to form a shell-like structure with 4/3/2 octahedral symmetry [1,8–11]. The H-subunit has a dinuclear iron center consisting of A and B binding sites (Fig. 1) where the fast conversion of $\text{Fe}(\text{II})$ to $\text{Fe}(\text{III})$ by dioxygen (or hydrogen peroxide) occurs, whereas the L-subunit is thought to contribute to the nucleation of the iron core and thus stores iron at a lower rate compared to the H-subunit [1,8–11,23]. The distribution of the H/L subunit ratio is tissue specific where up to 70% H subunits can be found in tissues exhibiting high ferroxidation activity (i.e., heart and brain) and up to 90% L subunits are found in tissues having mainly a storage function and much less iron oxidation activities (i.e., spleen and liver) [8,10]. More specifically, iso-ferritins from the following tissues are composed of these H to L ratios: human placenta ($\sim 20\%$ H, 80% L), human spleen ($\sim 10\%$ H, 90% L), human liver ($\sim 50\%$ H, 50% L), human heart ($\sim 90\%$ H, 10% L), human serum ($\sim 0\%$ H, 100% L), horse spleen ($\sim 8\%$ H, 92% L), and rat liver ($\sim 35\%$ H, 65% L) [8,24]. Exclusively homopolymer ferritins (i.e., H-type in bacterial ferritins, mammalian mitochondrial ferritins, and M-type in fish and amphibian ferritins) seem to be able to carry out both reactions of iron oxidation and iron mineralization [25–27].

2.2. Ferritins and ferritin-like proteins in bacteria

In bacteria, there are at least three types of iron storage proteins: the archetypal ferritins, the heme-containing bacterioferritins, and the Dps proteins [6]. The archetypal ferritins are similar to those found in eukaryotes and are composed of the typical but identical 24 homopolymer H-type subunits. The bacterioferritins are found only in eubacteria and consist of 24 identical H-subunits and up to 12 protoporphyrin IX heme groups of unknown function [28,29]. In *Escherichia coli*, these latter bind covalently between 2-fold symmetry-related subunits and are ligated by methionines Met-52 and Met-52'.

The Dps proteins are present only in prokaryotes and are smaller compared to ferritin (i.e., ~ 250 kDa vs. ~ 500 kDa). They consist of only 12 similar subunits organized in 3/2 octahedral symmetry and can accumulate just ~ 500 iron atoms per protein shell [30]. Interestingly, all three protein types can exist in the same bacterium but bind and oxidize iron quite differently. In the 24-mer proteins, the ferroxidation reaction takes place at conserved amino acid residues located within the H-subunit, whereas iron oxidation in Dps occurs at sites located at the 2-fold interface between the two subunits [30]. Each ferritin subunit is folded into four α -helix bundles (helices A–D) with helices B and C connected by a loop L that traverses the length of the bundle and a short fifth helix E (Fig. 1) that ends at the C-terminal [1,8–11]. Plant and animal ferritins share a high amino acid sequence homology and a very similar 3D structure with, however, two major differences that are related to localization and expression. Firstly, animal ferritins are localized in the cytoplasm of cells whereas plant ferritins are found in the plastids, a family of specific plant organelles responsible for the proper functioning of the plant (refer to the chapters by Zhao and by Briat et al. in this special BBA issue). Secondly, animal ferritins are mainly expressed and regulated at the translational level, whereas plant ferritins are regulated at the transcriptional level [4].

3. Ferritin channels

3.1. Vertebrate channels

In most species, the assembled 24 subunits in ferritin are tightly packed together leaving eight narrow hydrophilic channels around

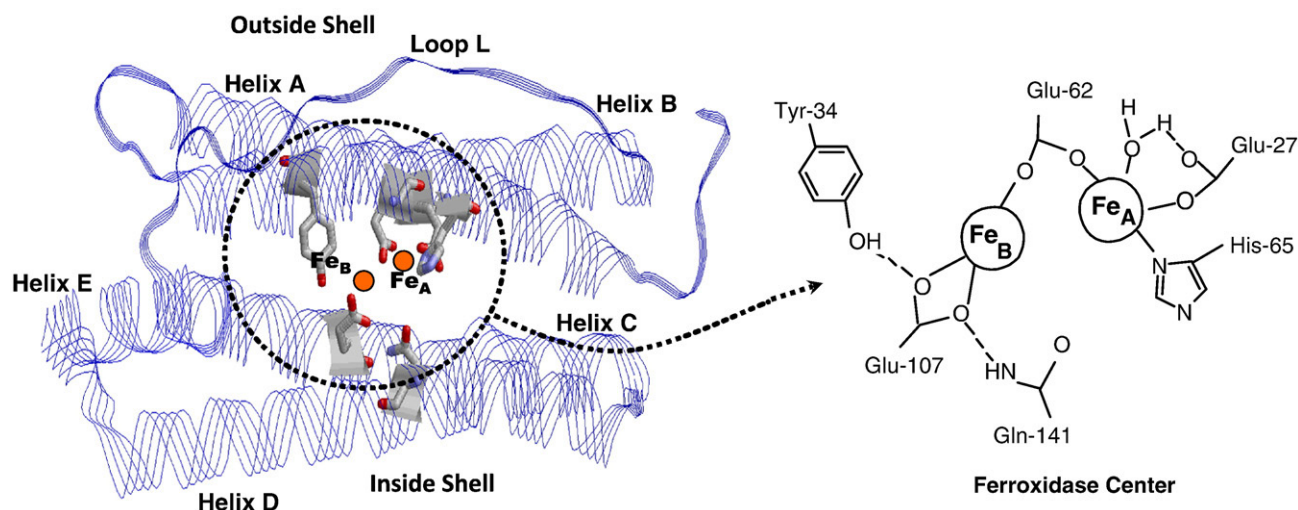


Fig. 1. Schematic view of the di-iron ferroxidase center on the four-helix of the H-chain ferritin (left panel). Dinuclear ferroxidase center diagram (right panel) showing residues from the Tb-derivative X-ray structure of ferritin. Adapted from Bou-Abdallah et al. [35] and Toussaint et al. [89].

the 3-fold axes and six hydrophobic channels around the 4-fold axes (Figs. 2b and a, respectively) both about 4 Å wide in diameter [8–11]. Most data indicate that iron enters and exits the cavity of animal ferritins via the eight hydrophilic 3-fold channels [31–35], while the hydrophobic channels are thought to be involved in diffusion of oxygen and hydrogen peroxide [22,36], although long-range electron tunneling mediated by aromatic groups within the protein shell has been suggested [37]. Recent calculations of electrostatic potentials, molecular diffusion, and thermodynamic and kinetics measurements of animal ferritin reinforced this proposal and illustrated the permeability of the protein's 3-fold channels to small ligands and molecules [32,36,38–40]. Alterations of the conserved amino acid residues that line these channels (aspartate and glutamate residues) decreased the capacity of H-chain ferritins to bind and oxidize Fe(II). Inhibition kinetics experiments employing Zn(II) and Tb(III) as probes of Fe(II) oxidation indicated that the mechanism of inhibition occurs through blocking the passage of Fe(II) to the ferroxidase center, suggesting that the 3-fold channels are the main pathway of iron(II) entry in ferritin [31]. Binding experiments using Mn(II), VO(IV), Cd(II), Zn(II), and Tb(III) have shown that these metal ions compete with Fe(II) and Fe(III) and with one another, implying the existence of common binding sites for all these metal ions on the protein. Observed binding stoichiometries in conjunction with X-ray crystallography, Mössbauer, and EPR spectroscopy suggest several types of binding sites, at least one of which is located inside the 3-fold channels. Other classes of binding sites involving the ferroxidation and nucleation sites, the external surface of the apoprotein, residues such as His118, His128, Cys130, and other carboxyl groups within the protein shell, have also been identified and proposed as loci for metal ion binding [31, and references therein]. Fig. 3 illustrates the putative pathway into the protein via the 3-fold channel where residues Thr135, His136, and Tyr137 are proposed to be involved in guiding iron from the inner opening of the channel to the ferroxidase centers of the protein.

A recent investigation of the kinetics and pathways of Fe(II) and O₂ diffusion into human ferritin (HuHF) indicated that Fe(II) diffusion from the outside of the protein to the ferroxidase centers exhibited a half life of about 3 ms and involved a facilitated diffusion process [35]. The eight 3-fold hydrophilic channels were demonstrated to be the only avenues for rapid Fe(II) access to the ferroxidase center, whereas O₂ diffusion kinetics were too fast to be followed [35]. Other small molecules such as reductants/oxidants and iron chelators can also enter and leave the ferritin shell during the processes of iron

deposition and release (see the chapter by Watt et al. in this special BBA issue). Interestingly, modification of the region around the 3-fold channels (i.e., site-directed modifications of amino acid residues, chaotropic agents, and specific binding of small peptides) has been shown to have a significant positive effect on the rates of iron release from ferritin, suggesting an important role of these channels in modulating ferritin iron entry and exit [40–42].

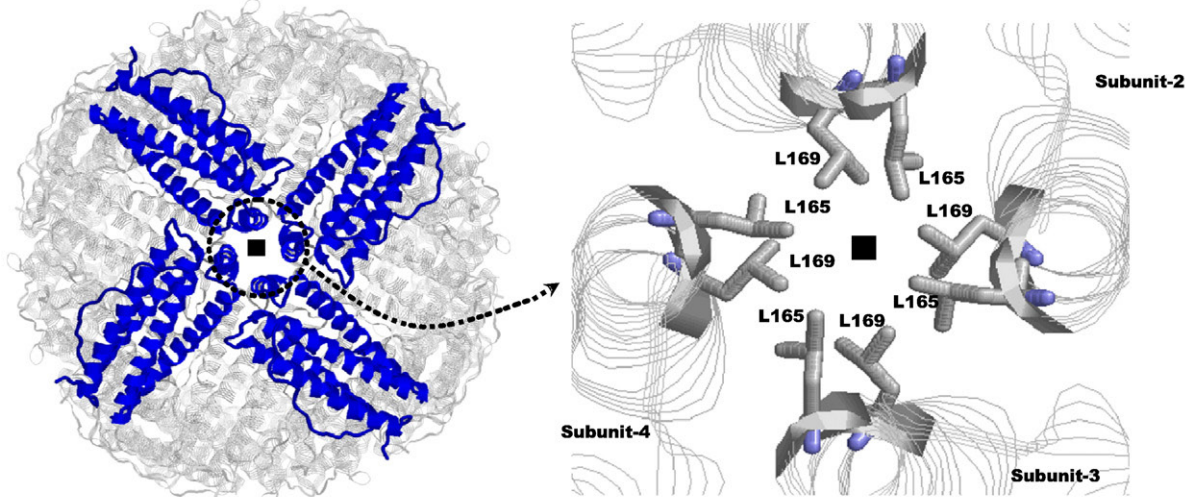
3.2. Invertebrate channels

Unlike vertebrate ferritins, the 3-fold channels in the heme (EcBFR) and nonheme (EcFtnA) ferritins from *E. coli* [43,44], the bacterioferritin from *Azotobacter vinelandii* [45,46] and the archaeal hyperthermophile and anaerobe *Pyrococcus furiosus*, PffTn [47], and *Archaeoglobus fulgidus*, AffTn [48], are less hydrophilic, while the 4-fold channels are more polar and a likely route of iron entry and release. Because of the alternating distribution of positively and negatively charged residues along the 3-fold and 4-fold channels, molecular surface and electrostatic potentials calculations suggested that iron might gain access to the inside of the bacterioferritin from *Desulfovibrio desulfuricans* (DdBf) by other channels located in between the 3- and 4-fold channels [49,50].

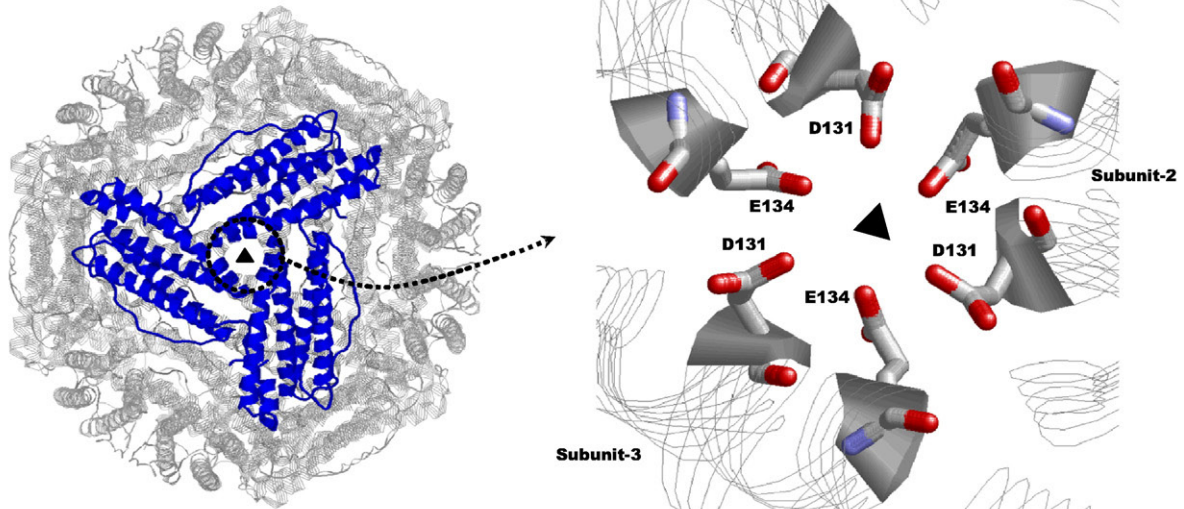
4. Ferritin ferroxidase centers

As mentioned earlier, the catalytic activity of ferritin is associated with the presence of a dinuclear A and B metal-binding site in each H or H-type subunits but not in the L-subunits [8,9,11,35]. This di-iron center called the “ferroxidase center” plays a critical role particularly during the early stages of iron oxidation and mineralization in ferritin (Table 1). It has been shown that the H- and L-subunits have complementary roles in iron oxidation and mineralization with maximum activity observed at a 30% H-subunit content (i.e., ~7 H and 17 L) [51,52]. The presence of a small number of L-subunits per ferritin molecule appears to modulate the ferroxidase activity of the H-subunits by accelerating iron translocation from the di-iron center into the cavity. Substitution of key residues at the dinuclear center leads to a great reduction of ferroxidase activity [51,53]. Interestingly, the ferroxidase centers of the handful of bacterial ferritins examined thus far (*P. furiosus* [47], *A. fulgidus* [48], and *E. coli* [44]) include a third iron-binding/oxidation site called the “C-site” that is somewhat unique to these proteins (Scheme 1). The exact role of this third C-site remains unknown, although a recent study suggested a possible function in shuttling electrons to a stable di-iron ferroxidase

A) 4-fold axis



B) 3-fold axis



C) 2-fold axis

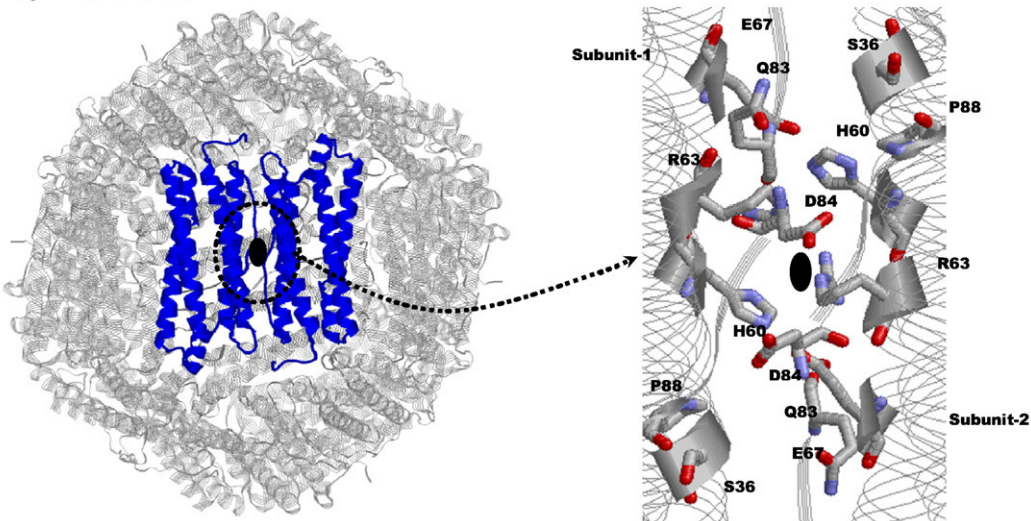


Fig. 2. Full ferritin shell (left panel) and expanded views (right panel) of three channel types: (A) 4-fold, (B) 3-fold, and (C) 2-fold channels with key residues indicated. The rotation symmetry related subunits is highlighted in blue in the left panels. Adapted from Bou-Abdallah et al. [35].

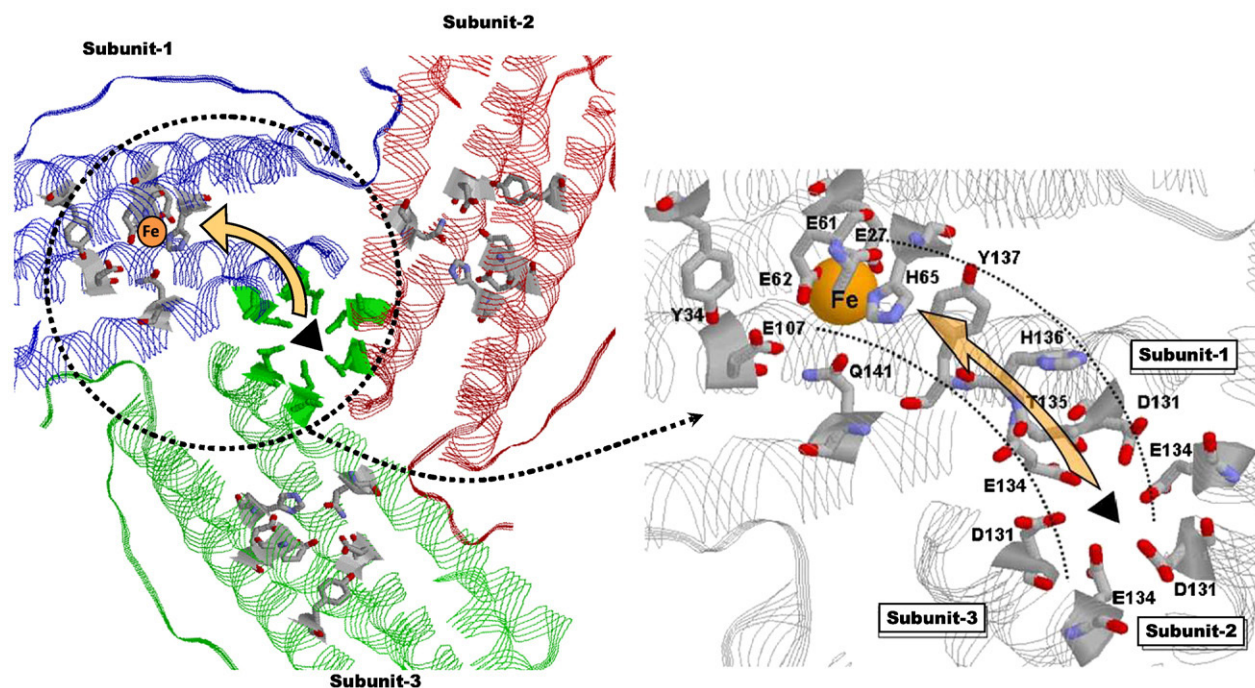


Fig. 3. Internal view of the three-fold channel of ferritin (left panel). The right panel shows a putative Fe(II) pathway from the three-fold channel to the ferroxidase center of the protein. Adapted from Bou-Abdallah et al. [35].

center [54]. As discussed in detail below, the latter acts as a stable catalytic center for the oxidation of incoming Fe(II) and their subsequent transfer to the protein's cavity to further build the iron core. The low occupancy of iron at the dinuclear ferroxidase centers of some of these ferritins as seen in the X-ray structures and the movement of conserved amino acid residues were explained in terms of a dynamic migration mechanism of iron from these sites to the inner cavity of the protein to form the mineral core. A detailed analysis and comparison of the X-ray structures of the di-iron ferroxidase centers of a number of ferritins, the overall subunit structure, and the subunit–subunit interactions is covered in a separate chapter of this special issue by Crichton et al.

5. Iron(II) oxidation at the dinuclear centers of ferritin: The role of the H-chain

A large number of *in vitro* studies have been carried out in the past three decades in an effort to understand the mechanism of iron oxidation and deposition in ferritins. The overall and generally accepted multistep mechanism involves the binding of ferrous ions at the protein catalytic sites followed by oxidation and movement of the resulting ferric ions into the protein cavity where a stable nucleus of crystalline mineral (ferrihydrite) starts to form. The growing mineral core then provides additional nucleation sites onto which incoming Fe(II) can be further deposited and oxidized. Under conditions of low iron fluxes (i.e., ≤ 48 Fe atoms/molecule, an amount required to saturate the 24 di-iron centers on each ferritin molecule), the protein catalytically oxidizes all 48 Fe(II) at these centers and virtually nothing reaches the cavity at this first stage of iron oxidation. As more and more iron enters the protein and once a mineral core is formed, another mechanism involving oxidation on the surface of a growing mineral occurs.

Because conserved amino acid residues at either the A or the B sites are critical for rapid iron binding and oxidation, a recent study showed that it is possible to reconstitute a dinuclear ferroxidase center in the inactive L-chain ferritin and obtain a protein with varying degrees of iron oxidative activity depending on the identity of the amino acids at these sites [22]. Ferritins with a reconstituted site A alone had no ferroxidase activity, whereas ferritins with both A and B sites showed equivalent catalytic activity to wild type ferritins. Earlier

kinetics and thermodynamic measurements of Fe(II) binding and oxidation in human and bacterial ferritins showed a preferred order of binding where Fe(II) binds first at site A and then at site B followed by dioxygen binding to site B and the formation of the first detectable μ -1,2-peroxodi-Fe(III) intermediate [32,55]. The weaker B site in ferritin is probably why differences have been observed in iron reaction intermediates between ferritins and di-iron carboxylate oxygenases (i.e., a labile peroxy/oxo/hydroxy di-iron(III) in ferritin *versus* a stable di-iron cofactor in oxygenases), although the effect of second shell amino acids in modulating the chemistry of iron oxidation at the dinuclear ferroxidase center is not ruled out. A recent study employing M-chain ferritin reported evidence for a model of concerted binding of two Fe(II) at the active site independent of the levels of iron loading. Such a discrepancy could be accounted for by the presence of different amino acid residues at the ferroxidase centers of the two proteins (i.e., a nonbinding alanine residue at site B of H-chain ferritin compared to a binding aspartate residue in M-chain ferritin). A μ -peroxy di-iron(III) intermediate is observed in some but not all ferritins despite the high degree of similarities in their amino acid sequences and their highly conserved structures and ferroxidase site residues (Table 1). The blue peroxy intermediate ($\lambda_{\max} \sim 650$ nm) has not been observed in EcBFR and the H-chain from recombinant frog ferritin [56,57], whereas in HuHF, HoSF, M-chain from recombinant frog ferritin, EcFtnA, and MtF, the blue complex has been readily detected by stopped-flow spectrophotometry [26,27,57–60]. In addition, the H_2O_2 that is produced at the dinuclear ferroxidase centers is used differently by these ferritins; EcBFR quickly consumes one H_2O_2 to oxidize two Fe(II) at a second di-iron site [61], whereas in other ferritins, it accumulates to measurable amounts in solution [57–63]. In HuHF, two Fe(II) ions are oxidized by one H_2O_2 , a stoichiometry that helps avoid the generation of hydroxyl radicals, whereas MtF lacks this $Fe^{2+} + H_2O_2$ detoxification property [26,53]. In ferritins where Fe(II) oxidation by O_2 produces a peroxy complex, the intermediate quickly decays to the more stable μ -oxo diferric complex with the concurrent release of H_2O_2 in solution (Scheme II). The resulting oxo/hydroxy ferric iron slowly translocates to the interior cavity of the protein where it is stored as a mineral resembling ferrihydrite in animals or as a ferric phosphate in bacteria [64].

Table 1
Representative ferritin types and their iron oxidation properties.

Ferritin name	Subunit composition	Preferred oxidant	Fe(II)/O ₂ ^a	A and B ferroxidase site ligands	Peroxo complex observed	Ferroxidase activity/iron turnover	References
HuHF: Human H-chain ferritin	24 H-subunits	O ₂ and H ₂ O ₂	2–4	E27, E62, H65, E107, Q141	Yes	Yes/yes	[57,82,89,94,96,97]
HuLF: Human L-chain ferritin	24 L-subunits	H ₂ O ₂	2.6–4	Y27, Y34, K62, G65, E107, E141	No	No/no	[53,70,82,92]
MtF: Mitochondrial ferritin	24 H-like subunits	O ₂ and H ₂ O ₂	2–4	E27, E62, H65, E107, Q141, S144	Yes	Yes/no	[26,91]
HosF ^b : Horse spleen ferritin	~ 21 L- and ~ 3 H-subunits	H ₂ O ₂	2–4	Y27, Y34, K62, G65, E107, E141	Yes	Yes/no	[58,68,92,97]
M-chain: Bullfrog ferritin	24 H-like subunits	O ₂ (no data available with H ₂ O ₂)	2	E23, E58, H61, E103, Q137, D140	Yes	Yes/yes	[27,63,70,87,90]
PfFtn: <i>Pyrococcus furiosus</i> ferritin	24 H-like subunits	O ₂ (no data available with H ₂ O ₂)	2–3.6	E17, E50, H53, E94, E130	ND	Yes/no	[47,54]
AvBF ^c : <i>Azotobacter vinelandii</i> ferritin	24 H-like subunits	O ₂ and H ₂ O ₂	4	E18, E47 ^d , E51, H54, E94, E127, H130 ^d	Yes	Yes/ND	[45,46,82,83]
DdBF ^c : <i>Desulfovibrio desulfuricans</i> ferritin	24 H-like subunits	O ₂ (no data available with H ₂ O ₂)	4	E23, E56, H59, E99, E132, H135	ND	ND	[49,88,95]
EcBFR ^c : <i>Escherichia coli</i> ferritin	24 H-like subunits	H ₂ O ₂	4	E18, E51, H54, E94, E127, H130	No	Yes/no	[29,61,76,93]
EcFtnA: <i>Escherichia coli</i> ferritin	24 H-like subunits	O ₂ (no data available with H ₂ O ₂)	3–4	E17, E50, H53, E94, E130	Weak	Yes/no ^e	[44,60,94]

ND = not determined.

^a Depending on the conditions and the ratio of Fe/protein used.

^b The amino acid residues forming the ferroxidase center on the H-subunit are conserved and are the same as in HuHF.

^c These ferritins contain 12 hemes per 24 subunits that are covalently bound between 2-fold symmetry-related subunits.

^d Not direct coordinating ligands but are involved in iron shuttling from the FC to the cavity.

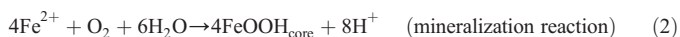
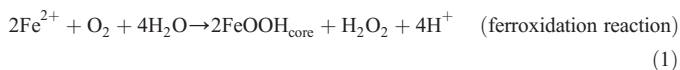
^e This work and unpublished results.

Interestingly, ferritin-like proteins (i.e., Dps) selectively use H₂O₂ over O₂ to oxidize iron at their catalytic di-iron centers with, on average, about 100-fold increase in the rate of iron oxidation compared to O₂ (refer to the chapter by Chiancone et al. in this special issue for further detail about Dps and its detoxification properties).

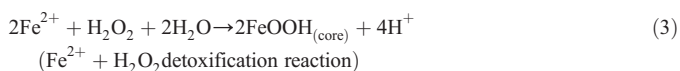
6. The mechanism of Fe(II) oxidation in recombinant human H and L ferritins, HoSF and BfMF

6.1. Historical models of Fe(II) deposition

Two models of Fe(II) oxidation in ferritin were originally proposed: the protein catalysis model and the crystal growth model [65,66]. More recent experiments using spectroscopy and stoichiometries of oxygen and proton uptake and release showed a wide range of Fe(II)/O₂ and Fe(II)/H⁺ ratios depending on the experimental conditions [8,40,67,68, and references therein], suggesting a multistep and more complex iron oxidation mechanism. The two net oxidation reactions that describe the two original models can be written as:



A more recent study [53] identified a third reaction in which the H₂O₂ produced in reaction (1) is consumed in the following detoxification reaction:



It is still unclear whether Fe(II) binding to the dinuclear sites in ferritin occurs pairwise or in a stepwise fashion. Two alternative schemes for Fe(II) oxidation have been considered and involve either a 2-electron oxidation scheme or a two successive 1-electron oxidation scheme [8,69]. Support for the 1-electron oxidation mechanism came from kinetics

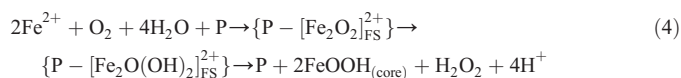
studies which indicated that the oxidation reaction was first order in both Fe(II) and O₂. In the 2-electron oxidation mechanism, 2 Fe(II) ions are simultaneously bound to the ferroxidase center of the protein followed by O₂ binding to one of the Fe(II) ions to form a di-Fe(III) species. In either scheme, the μ-peroxo di-iron(III) complex dissociates into a μ-oxo di-iron(III) intermediate and H₂O₂ is released (Scheme II).

6.2. Sequence of Fe(II) binding to the ferroxidase center A and B sites

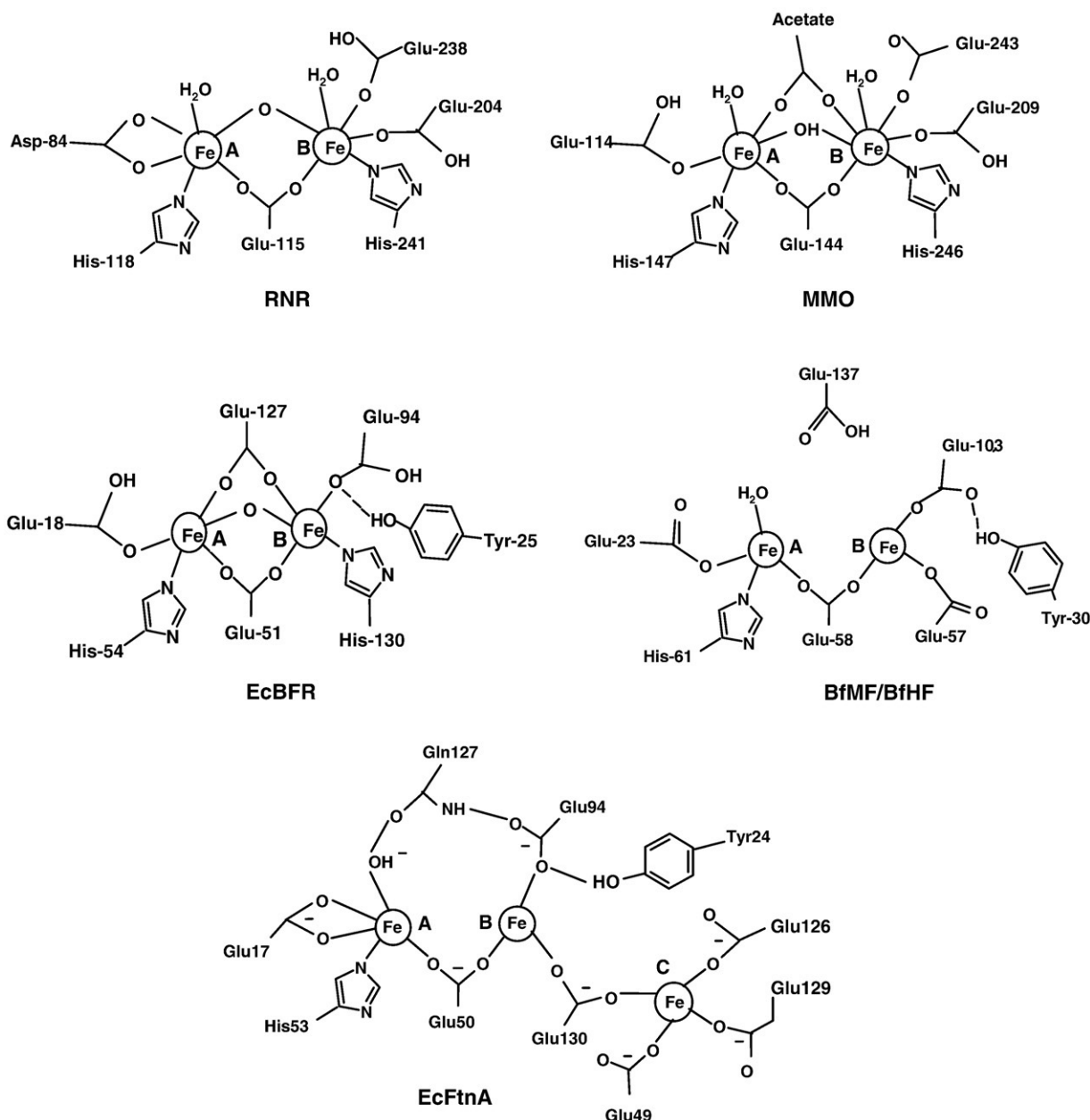
In further search for the early stages of Fe(II) binding to the dinuclear centers in ferritin and formation of transient iron–protein intermediates, an isothermal titration calorimetry (ITC) of Fe(II) binding to apoHuHF indicated that the ferroxidase center is the principal locus for Fe(II) binding and that the His65 containing A-site preferentially binds Fe(II) in accord with previous spectroscopic observations [32,40,55,70]. That only one site of the ferroxidase center is occupied by Fe(II) implies that Fe(II) oxidation to form di-Fe(III) species might occur in a stepwise fashion. Whether the binding of a second Fe(II) at the weaker B-site is required prior to oxygen binding and iron oxidation remains to be determined. Nevertheless, following Fe(II) binding at the ferroxidase center and at low flux of Fe(II) into human H-chain apoferritin (HuHF) (≤50 Fe(II)/protein), the iron is primarily processed by the di-iron ferroxidase center.

6.3. Ferroxidase center intermediates

The net ferroxidation/mineralization reaction occurs with an Fe(II)/O₂ stoichiometry of ~2:1, resulting in the production of hydrogen peroxide according to the following reaction sequence:



This H-chain iron-catalyzed oxidation reaction is similar to Eq. (1). However, it shows the two di-Fe(III) intermediates that are the precursors to the iron core, the μ-1,2-peroxodi-iron(III) intermediate designated P-[Fe₂O₂]_{FS}²⁺, where P represents a vacant ferroxidase site



Scheme I. Schematic representations of the dinuclear centers of RNR, MMO, EcBFR, BfMF/BfHF, and EcFtnA. The structures were drawn with ChemDraw (CambridgeSoft Corp., Cambridge, MA, USA).

(FS) on the H-subunit and the μ -1,2-oxodi-iron(III) intermediate(s) designated $P\text{-}[\text{Fe}_2\text{O}(\text{OH})_2]_{\text{FS}}^{2+}$ the decay product of the peroxo complex.

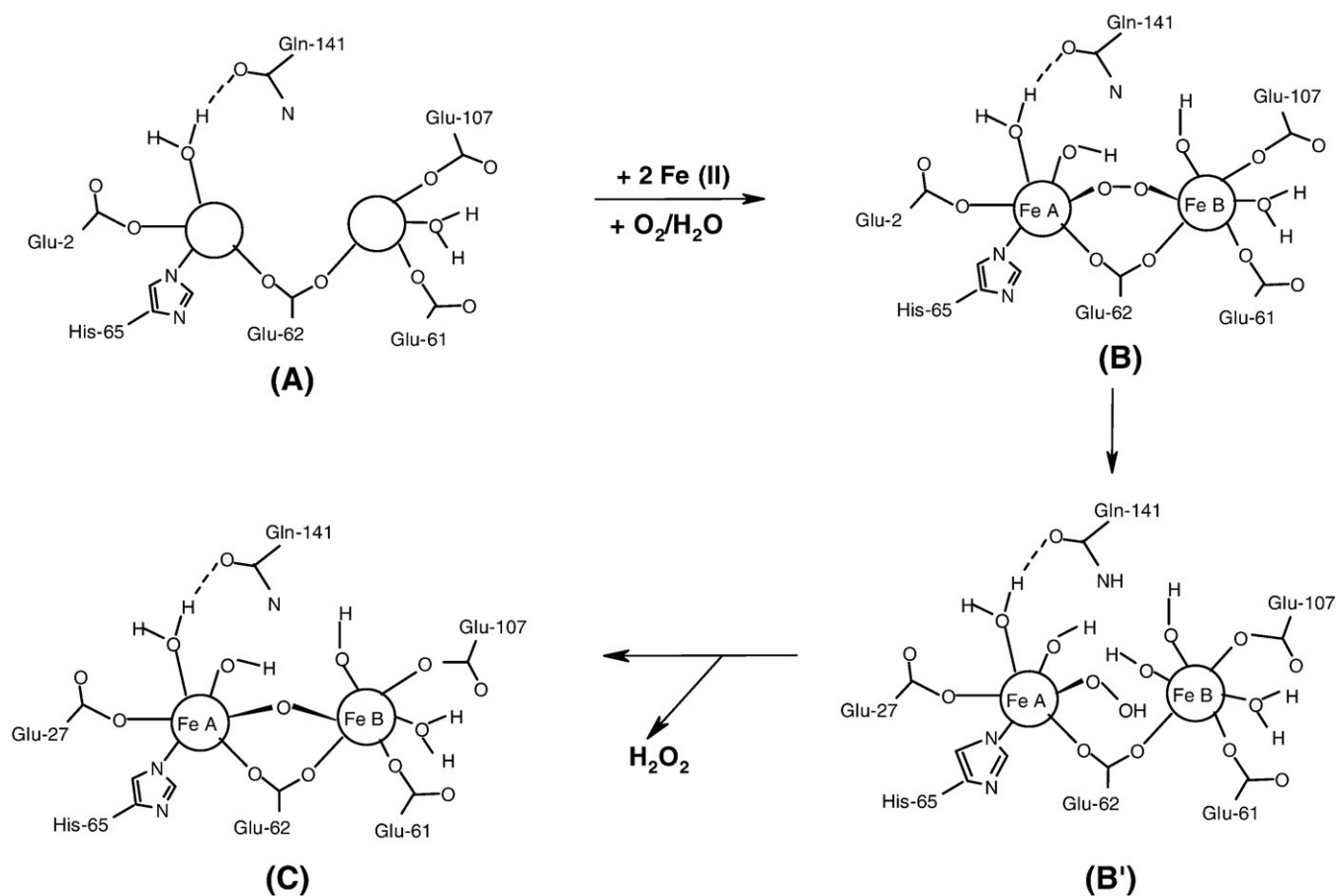
In accordance with Eq. (4), stopped-flow kinetics, resonance Raman spectroscopy, Mössbauer spectroscopy, and EXAFS have established that a μ -1,2-peroxodi-Fe(III) intermediate is formed during the first 50 ms of Fe(II) oxidation by O₂ at the ferroxidase site [62, and references therein]. This first intermediate subsequently decays within 150 ms to one or more μ -oxo(hydroxo)-bridged di-iron (III) intermediate(s) and small clusters whereupon H₂O₂ is produced in a stoichiometric amount and released into solution (Scheme II). The μ -oxo(hydroxo)-bridged di-Fe(III) dimer(s) and clusters ultimately lead to the formation of large polynuclear aggregates and the mineral core itself.

In various stopped-flow experiments employing different amounts of Fe(II)/protein, unusually complex kinetics behavior has been reported [53,62]. A catalytic model for the unusual features of

the oxidation/mineralization processes has been developed and demonstrated that the ferroxidase site of the protein is involved in iron oxidation at all levels of iron loading. A new transient species, postulated to be a hydro-peroxodi-Fe(III) complex was suggested to be the decay product of μ -1,2-peroxodi-Fe(III) complex (Scheme II).

6.4. Mineral surface and detoxification reactions

When a larger flux of Fe into the protein is used, the iron oxidation mechanism changes from essentially a ferroxidation reaction $\{2 \text{Fe(II)}/\text{O}_2, \text{Eqs. (1) and (4)}\}$ to a combination of ferroxidation, mineralization and $\text{Fe}^{2+} + \text{H}_2\text{O}_2$ detoxification reactions [Eqs. (1)–(3)]. Reaction (2) is the dominant reaction at $\sim 800 \text{ Fe(II)}/\text{protein}$, whereas reaction (3) occurs largely at intermediate iron loadings of 100–500 Fe(II)/protein [53]. Under conditions of high Fe/protein ratios, the Fe(II)/O₂ stoichiometry approaches 4:1 (Table 1), and dioxygen is ultimately



Scheme II. Ferroxidase center reaction intermediates in H-chain ferritin. (A) apoprotein, (B) μ -peroxy di-iron(III) complex, (B') μ -hydroperoxy di-iron(III) complex, and (C) μ -oxo di-iron(III) complex.

reduced to water according to Eq. (2). Since Eq. (2) is identical to that of Fe(II) autoxidation and hydrolysis, it has been assumed that core mineralization at high Fe(II) fluxes likely occurs through iron deposition directly on the surface of the mineral according to the crystal growth model. An incipient core of 200 Fe(II) per protein appears to be the minimal size for reaction (2) to occur appreciably [53]. Human L-chain ferritin (HuLF) and H-chain (HuHF) variants lacking functional ferroxidase sites deposit their iron largely through the mineral surface reaction (2) where H₂O₂ is shown to be an intermediate product of dioxygen reduction. HuLF and HuHF ferroxidase center variants display sigmoidal kinetics representative of a mineral surface process whereby the slow initial phase of the sigmoidal curve represents nucleation and development of the incipient core upon which the autocatalytic mineral surface reaction ensues [53]. It is conceivable that reaction (2) is a combination of reactions (1) and (3), which lead to an overall reaction stoichiometry of 4 Fe(II)/O₂ and 2 H⁺/Fe(II) as determined by oximetry and pH-stat measurements.

6.5. Similar overall structure but different kinetics and iron intermediates

Despite the similarities of the ferroxidase sites and the ability of many ferritins including HuHF, BfMF, and HoSF to efficiently form an iron core, there are marked differences in the detail of the oxidation mechanism and the intermediate iron species generated. In all three proteins, a blue peroxo di-iron(III) complex ($\lambda_{\max} = 650$ nm and $\epsilon = 850\text{--}1000$ M⁻¹ cm⁻¹ per dimer) is rapidly formed within the first few milliseconds (25–100 ms) of mixing Fe(II) and O₂ (formation rates $k_1 \sim 80$ s⁻¹ for HuHF and BfMF and ~ 18 s⁻¹ for HoSF and decay

rates $k_2 \sim 2.8$ s⁻¹ for HuHF, ~ 4.2 s⁻¹ for BfMF, and ~ 1.5 s⁻¹ for HoSF) [27,58,59,62,63,74]. Whereas no detailed kinetics data are available for BfMF, at higher Fe loading of HuHF and HoSF (~ 20 Fe(II)/H-subunit), an absorbance plateau developed in HuHF but not in HoSF. The appearance of the plateau in HuHF indicated equal rates of the peroxo complex formation and decay as iron is turned over continuously at the ferroxidase site. This observation provided direct evidence that the catalytic activity of the ferroxidase site is maintained at all levels of Fe(II) loading of the protein (Fig. 4). The lack of such plateau in HoSF indicates a different mechanism of fast Fe(II) oxidation and a lack of the catalytic turnover of iron and instant regeneration of ferroxidase activity. Nevertheless, the initial and rapid oxidation of Fe(II) in HoSF appears to be an important first step that provides a small Fe(III) nucleus upon which further oxidation and building of the mineral core occurs via essentially an autocatalytic process. Moreover, unlike HuHF and HoSF where only a single oxo(hydroxo) dimer is evident in the first 10 s of the Fe(II) oxidation reaction, the peroxo complex of bullfrog ferritin decays to multiple oxo(hydroxo) dimers and small clusters within the first few seconds. Multiple dimers and clusters do not appear in HuHF and HoSF until minutes later [57,58,63]. In horse spleen ferritin, the slower iron oxidation kinetics is consistent with the fact that the L-subunits are responsible for long-term storage of iron through the slow process of mineralization.

6.6. Natural heteropolymer ferritins

With the exception of serum ferritin and mitochondrial ferritin, heteropolymer ferritins of various H to L ratios are widely distributed in mammalian cells and seem to be biologically more favored where

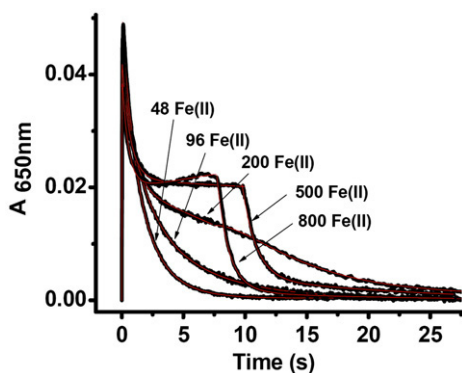


Fig. 4. Stopped-flow kinetics (black) and simulated curves (red) for different iron loadings into human H-chain ferritin. Adapted from Zhao et al. [53].

up to 25 possible isoferritins can exist, the two homopolymers (24 H- or 24 L-subunits) and the 23 possible combinations in between [8]. The horse spleen ferritin (HoSF), a native heteropolymer composed of about 85% L-chains and 15% H-chains, takes up Fe(II) a lot faster than the recombinant homopolymer L-chain, which, despite the lack of a functional ferroxidase center, can still oxidize Fe(II) albeit at a much slower rate [58]. The fast iron oxidation activity of HoSF (compared to homopolymer L-chain) is presumably due to the presence of a few H-chains (~ 3 on average; Table 1). However, this ferroxidase activity on a per H-chain basis is significantly different from that predicted considering the H/L subunit ratio alone [71], suggesting a cooperative interaction between the L- and H-subunits in forming the mineral core. Indeed, the iron oxidation mechanism in HoSF is different from that of the homopolymer analogues (more below).

6.7. Synthetic heteropolymers

In an ongoing investigation using two recombinant heteropolymer ferritins (ca. ~ 20 H/4 L and ~ 22 L/2 H), it was found that the L-chain facilitates iron turnover at the ferroxidase center of the H-subunit in the ~ 20 H/4 L protein (Bou-Abdallah et al., unpublished results). Iron oxidation occurs mainly on the H-subunit with a stoichiometry of 2 Fe(II):1 O₂, suggesting the formation of H₂O₂. However, unlike in HuHF where most of the H₂O₂ produced at the ferroxidase center subsequently reacts with further Fe(II) (Eq. (3)), most of the H₂O₂ produced in the recombinant heteropolymer H/L (~ 20 H/4 L) remains in solution. In addition, the ~ 20 H/4 L heteropolymer (but not the ~ 22 L/2 H heteropolymer) completely regenerates its ferroxidase activity within a short period (less than an hour), suggesting rapid movement of Fe(III) from the ferroxidase center to the cavity to form the mineral core. In the L/H heteropolymer (~ 22 L/2 H), Fe(II) oxidation appears to occur by two simultaneous pathways: (1) a ferroxidation pathway with a 2 Fe(II)/1 O₂ ratio and a mineralization pathway with a 4 Fe(II)/1 O₂ resulting in an average net stoichiometry of ~ 3 Fe(II)/1 O₂. Thus, in the L/H heteropolymer, the H-subunit appears to be involved at all times in iron oxidation and mineral core formation (Bou-Abdallah et al., unpublished results), although the overall rate of iron oxidation is significantly slower than that observed in the H/L heteropolymer. Nevertheless, it has been found that iron cores in recombinant L-ferritins and native heteropolymers are slightly larger in size, more crystalline, and better magnetically ordered than those in H-chain ferritin as viewed by electron microscopy, suggesting that the L-chains are better at ferrihydrite nucleation [72,73].

The behavior observed with the 22 L/2 H heteropolymer is similar to that reported for HoSF, whereas that with the 20 H/4 L sample is similar

to that reported for HuHF, indicating that the synthetic heteropolymers behave similarly to the natural proteins. It appears that the presence of a few L-chains in heteropolymer ferritins has an important effect on the rapid turnover of iron at the FC of the H-chains. In contrast, the presence of too many L-chains appears to change the iron oxidation mechanism to a two-step process involving ferroxidation (i.e., at 2 Fe(II)/O₂) and mineralization (i.e., 4 Fe(II)/O₂) as suggested by the observed net oxidation stoichiometry of ~ 3 Fe(II)/O₂. The rate of iron oxidation at the FC of the L/H heteropolymer (~ 22 L/2 H) ferritin is about 15- to 20-fold slower than that of the H/L heteropolymer (~ 20 H/4 L). In the case of the L/H heteropolymer, the effect of the L-chain on the iron turnover cannot be easily discerned presumably because of the presence of very few H-chains. In contrast, the homopolymer H-chain itself can slowly turnover its iron at the FC, requiring many hours for complete iron clearance compared to less than 1 hour for the heteropolymer ~ 20 H/4 L ferritin. However, additions of large amounts of iron to the homopolymer H-chain at once (i.e., 500 Fe(II)/shell) appears to accelerate iron turnover as indicated by the kinetic data described above [62].

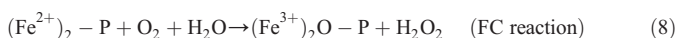
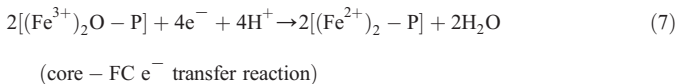
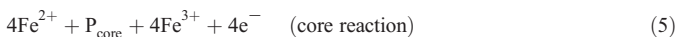
7. The mechanism of Fe(II) oxidation in bacterial (EcBFR, EcFtnA) and archaeal (Pfftn) ferritins

The *E. coli* bacterium produces at least two true ferritins (and one ferritin-like protein called Dps (DNA binding proteins from starved cell) with fast iron ferroxidation reactions: a heme (EcBFR) and a nonheme ferritin (EcFtnA). A third nonheme ferritin type (EcFtnB) lacks the fast iron oxidizing property, and it is not known whether it has an iron storage function [75,76]. EcFtnA is similar to human H-chain ferritin (HuHF) (i.e., 24 identical H-type subunits constitute the protein shell) but has an additional third iron-binding site (C-site) that is unique to this protein and is ~ 7 Å away from the B-site and ~ 11 Å from the A-site [44,77] (Scheme 1). Similarly, the ferritins of the hyperthermophilic archaeal anaerobes, *P. furiosus* (Pfftn) and *A. fulgidus* (Afftn) have 24 identical H-type subunits with 24 di-iron ferroxidase centers and one additional third iron C-site on each subunit [47,48].

7.1. Fe(II) binding and oxidation stoichiometries in EcBFR

The iron oxidation mechanisms in the ferritins from *E. coli* (EcFtnA and EcBFR) and the ferritin from the hyperthermophilic archaeon *P. furiosus* (Pfftn) do not seem to follow the iron oxidation mechanism discussed above for animal and amphibian ferritins. In Pfftn, a stable dinuclear complex resulting from the oxidation of the first 48 Fe(II)/protein at the ferroxidase center of the protein is formed. Unlike in animal ferritins where an active ferroxidase center that is involved in nearly all stages of iron oxidation and core formation (and thus a regeneration of the ferroxidase activity over time), the di-Fe(III) complex in Pfftn [54] and EcFtnA (Bou-Abdallah et al., unpublished results) serves as a stable group where indirect catalysis of further incoming Fe(II) occurs. In Pfftn, the oxidized Fe(II) is transferred to the iron core which itself is not involved in the oxidation of Fe(II). However, in EcBFR, a di-Fe(III) ferroxidase complex acting as a stable catalytic cofactor acquires electrons from a core via a Fe(II) binding site that has been recently identified on the inside of the protein [78,79]. This novel iron site is on the inner surface of the protein and ~ 9 – 10 Å below the dinuclear ferroxidase center where iron is coordinated by only two residues, His46 and Aps50 [79]. More recent fluorescence quenching and Zn inhibition studies offered support to this proposal and suggested that iron core formation in EcBFR occurs through the ferroxidase center which acts as a true catalytic center whereby the di-iron ferroxidase complex is a stable entity that constantly cycles iron between the diferrous and the diferric forms [80]. Consistent with these observations, a mechanism has been proposed in which the initial binding and oxidation of two ferrous ions at the ferroxidase center of EcBFR is followed by the binding and

oxidation of more ferrous ions at acidic site residues and/or the surface of the growing mineral core and subsequent electrons transfer to the di-Fe(III) ferroxidase complex. The resulting diferrous ferroxidase center species of EcBFR is then oxidized by either O₂ or H₂O₂ according to the following stoichiometric reactions:



and the overall net stoichiometry is given by:



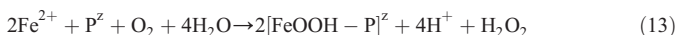
Here, P_{core} represents the acidic site residues and/or mineral core surface sites, (Fe²⁺)₂-P and (Fe³⁺)₂O-P represents the diferrous and diferric iron complexes at the ferroxidase centers, and [FeOOH]_{core} represents the iron mineral core. This mechanism is in agreement with earlier studies [29,61] where the stoichiometric equations corresponding to Fe(II) binding, oxidation, and hydrolysis in EcBFR have been determined using electrode oximetry/pH-stat and UV-visible absorbance measurements (Table 1). In these studies, the initial and rapid pairwise binding of 2 Fe(II) ions at a dinuclear ferroxidase site led to the release of 4 protons according to the following reaction:



The oxidation of the diferrous ferroxidase complex (Fe²⁺)₂-P by O₂ or by H₂O₂ corresponds to Eqs. (8) and (9), respectively [29,61]. While the overall mineralization reaction involving O₂ and H₂O₂ is given by Eq. (10), another mineral core formation reaction involving direct oxidation of Fe(II) by H₂O₂ at acidic site residues or directly on the surface of the growing mineral core can be written as:



Reactions (9) and (12) suggest that EcBFR is able to nullify the toxic combination of Fe(II) and H₂O₂ and thus minimize the production of hydroxyl radical, a result supported by EPR spin trapping experiments [61]. In addition, oximetry and pH-stat measurements [29,61] suggested that Eq. (10) can be simply written as a combination of two simultaneous reactions:

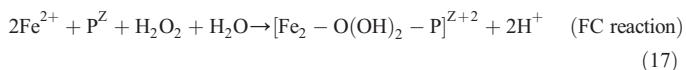
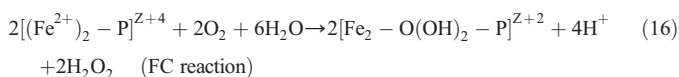
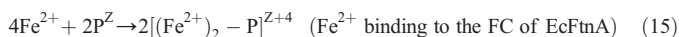


leading to an overall reaction stoichiometry of 4 Fe(II)/O₂ and 2 H⁺/Fe(II).

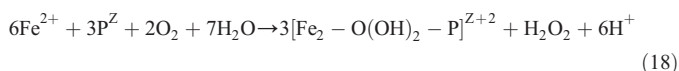
7.2. Fe(II) binding and oxidation stoichiometries in EcFtnA and PfFtn

Recent isothermal titration calorimetry (ITC) measurements of Fe(II) binding to EcFtnA [81] under anaerobic conditions indicated the presence of essentially two classes of binding sites with a stoichiometry of ~24 Fe(II) per class of sites at pH 7.0 (2 Fe(II) at each of the 24 dinuclear ferroxidase centers of the protein). The ITC data revealed that the C-site of EcFtnA is not involved in strong Fe(II) binding but appears to modulate Fe(II) binding at the adjacent dinuclear A and B iron sites. In addition, the data suggested a highly interactive ferroxidase center and the presence of inter- and intrasubunit negative cooperativity between Fe(II) binding at the various sites [81]. More recent experiments (Bou-Abdallah et al., unpublished data) employing oximetry/pH-stat and UV-visible and fluorescence spectroscopy indicated a binding stoichiometry of 48 Fe(III) per EcFtnA in accord with the ITC data. The presence of the C-site in EcFtnA causes the iron oxidation stoichiometry of the first 48 Fe(II)/shell added to increase from ~2 to ~3 Fe(II)/O₂, suggesting incomplete reduction of oxygen to water (Table 1). While the C-site is not required for fast oxidation of the first 48 Fe(II)/shell at the di-iron ferroxidase center of EcFtnA, three EcFtnA C-site variants (E49A, E126A, and E130A) exhibited a Fe(II)/O₂ stoichiometry of ~2:1 like that of human recombinant H-chain ferritin (HuHF), which lacks a C-site, indicating the involvement of C-site in oxygen redox chemistry.

Electron paramagnetic resonance (EPR) measurements indicate the formation of protein radical (likely involving Tyr34) following the oxidation of Fe(II) by O₂ (Bou-Abdallah et al., unpublished data). Because variant Y34F shows similar iron oxidation kinetics to wild type EcFtnA, this radical does not seem to be important for the protein-catalyzed oxidation of iron and probably is a by-product of oxygen radical chemistry. A mechanism for iron oxidation and mineral core formation in EcFtnA is proposed (see below) in which the C-site is suggested to play a role in hydrogen peroxide detoxification and in building of the mineral core through electron transfer from an Fe(II) at the C-site to the di-Fe(III)-protein complex at the ferroxidase center (Bou-Abdallah et al., unpublished data). A similar mechanism has been proposed for the hyperthermophilic archaeal anaerobe, *P. furiosus* (PfFtn), noted earlier in which a stable iron-containing ferroxidase center acts as a stable catalytic center whereby the dinuclear Fe(III)-center accepts two subsequent electrons from nearby Fe(II) ions at the C-site resulting in their oxidation. The oxidized iron leaves the C-site to the cavity and contributes to the building of the core while molecular oxygen is reduced to hydrogen peroxide to complete the cycle of the electron transfer chain. Note that the C-site in PfFtn [47] and in AfFtn [48] is similar to that found in EcFtnA [44] (Table 1 and Scheme 1). Accordingly, we write the following mechanism of iron binding and oxidation in EcFtnA as follows:



with a net reaction of:



where [(Fe²⁺)₂-P]^z represents a di-Fe(II)-protein complex at the A and B sites of the ferroxidase center as observed by ITC anaerobic titration of

EcFtnA with Fe(II) [81]. Eqs. (16) and (17) are two concurrent oxidation reactions occurring at the ferroxidase centers A and B of EcFtnA where $[\text{Fe}_2\text{-O}(\text{OH})_2\text{-P}]^{Z+2}$ represents a Fe(III)- μ -oxo-bridged di-iron(III) species. The above mechanism indicates that twice as much iron must be oxidized through Eq. (16) and only one-half of the H_2O_2 produced in Eq. (16) is utilized to oxidize additional iron through Eq. (17). Eq. (18) accounts for the observed Fe(II)/ O_2 and H^+ /Fe(II) stoichiometries of 3.0 and 1.0 obtained by oximetry and pH-stat, respectively. We suggest that reaction (17) takes place mostly at the ferroxidase center of the protein and to a lesser extent at the third C-site leading to the formation of small amounts of mononuclear iron species as demonstrated by EPR spectroscopy (Bou-Abdallah et al., unpublished results).

The mechanism discussed above for EcBFR probably applies to *A. vinelandii* bacterioferritin (AvBF) as well. A stoichiometry of 4 Fe(II)/ O_2 is observed in AvBF (Table 1) indicating the complete reduction of oxygen to water [46,82]. It is conceivable that in AvBF, H_2O_2 is a transient intermediate and does not accumulate in solution to detectable levels as shown in Eqs. (10), (13), and (14). Other mechanisms of iron oxidation and deposition in ferritins, which do not involve O_2 or the ferroxidase centers, have been proposed [83]. These alternative mechanisms employed large oxidants and long-range electron transfer reactions and have been suggested to help avoid unwanted secondary reactions that might otherwise involve damaging reactive oxygen species.

8. Oxygen versus hydrogen peroxide selectivity in ferritins and ferritin-like proteins

Many microbes regulate iron homeostasis in the absence of oxygen and thus might be a reminiscent example of early organisms that lived billions of years ago before oxygen was present [84]. Ferritin-like proteins (i.e., Dps) and some bacterial ferritins (i.e., EcBFR) preferably use H_2O_2 to oxidize ferrous iron and store the oxide as a mineral core inside the protein cage while animal ferritins use mainly O_2 as the iron oxidant. The preferential use of O_2 versus H_2O_2 in some ferritins might be an indication of an evolutionary pathway that required primordial life to accommodate to deal with iron and oxygen toxicity [85]. An excellent review article on the evolutionary pathway of ferritins and their diversion to distinct subfamilies is presented in a separate chapter of this special issue by S.C. Andrews.

While the exact structural basis of oxidant selectivity (O_2 vs. H_2O_2) remains unknown, the difference in iron ligands environment, second-shell or distant residues, and structure of the protein ferroxidase centers are structural reasons that might explain why certain ferritins prefer O_2 or H_2O_2 as the iron oxidant at the catalytic sites (Table 1). In all Dps proteins characterized thus far, a unique and conserved di-iron binding motif, located between two subunits rather than in the middle of the subunit as found in ferritins, serves to efficiently oxidize Fe(II) to Fe(III) using H_2O_2 and avoids the production of toxic hydroxyl radicals through the Fenton reaction (reviewed in this special issue by Chiancone and Ceci). The iron ligands at the ferroxidase center of EcBFR are homologous to those of the di-iron enzymes (i.e., two EXXH sequences) where the oxidized iron is retained at the di-iron centers of both proteins. In contrast, the ferroxidase centers of H-chain ferritins are more flexible allowing the movement of iron from the catalytic center to the protein's cavity. In EcBFR, each iron is coordinated by a histidine and a glutamate residue and bridged by two carboxylate groups (Scheme I), whereas in H-type ferritins, only one metal has a histidine ligand (Fig. 1). It has been suggested that the differences in the ferroxidase site ligands between ferritin and the dinuclear nonheme iron enzymes such as methane monooxygenase (MMO) and ribonucleotide reductase (R2) is one structural reason that could account for the differences in reaction pathways and reaction products of these proteins [86]. Particularly, the second Fe site in ferritin is weaker and different from that of nonheme iron enzymes in that only a single glutamate bridge exists at

the dinuclear center in ferritin compared to two glutamate bridges in the nonheme iron enzymes [86]. In addition, other non-conserved residues (i.e., aspartate, serine, and alanine in ferritins vs. a conserved histidine in iron enzymes), the presence of two coordinating water molecules at the dinuclear center in ferritin and weaker ligand field have also been suggested as important factors in determining reaction pathways and intermediates and the formation of either a stable cofactor as in MMO and R2 or a labile intermediate leading to mineral core formation as in ferritin [84,86].

9. Conclusions and perspectives

The ferritin-catalyzed ferroxidation reaction requires the copresence of Fe(II) and an oxidizing agent for the rapid and efficient initiation of the iron core within the protein shell. While the in vivo mechanism remains largely unknown, numerous studies have examined the mechanism of Fe(II) entry, oxidation, and deposition in ferritin in vitro (Table 1). In contrast, relatively fewer studies have been directed at elucidating the iron mobilization mechanism. In either case, the ferritin channels are shown to be flexible structures that allow the entry and exit of different molecules of varying sizes. Iron oxidation and core formation begin at di-iron sites within each of the 24 protein subunits with Fe(II)/ O_2 ratios varying between 2 and 4. The ferroxidation reaction of most ferritins produces H_2O_2 as a by-product of O_2 reduction. The latter either accumulates in solution to measurable levels or is rapidly used by the protein to oxidize additional Fe(II) with minimal production of hydroxyl radicals. Interestingly, some ferritins (EcBFR) or ferritin-like proteins (Dps) preferentially use H_2O_2 over O_2 as the iron oxidant to form the iron core (Table 1). The ferroxidase site ligands in ferritins are similar to those found in the di-iron cofactor sites of methane monooxygenases, fatty acid acyl desaturases, and ribonucleotide reductases. However, iron is a substrate in ferritin but a cofactor in the di-iron cofactor proteins. In addition, the product of iron oxidation at the ferroxidase centers of ferritin is labile and is retained in the protein cavity in the form of a mineral core, whereas the iron complex in the di-iron cofactor proteins is stable and remains at the catalytic site. It appears that those proteins that prefer H_2O_2 over O_2 as the iron oxidant do not turn over the oxidized iron as is the case with H-chain like ferritins (Table 1). It was suggested that the difference in the identity of the ferroxidase center ligands and the iron binding affinity particularly of the B sites might influence the distinct reaction pathways between ferritin and the di-iron cofactor enzymes [87]. Nevertheless, the rapid reaction of Fe(II) with dioxygen produces initially a peroxo di-iron(III) intermediate in both ferritin and the di-iron cofactor proteins. While a stable high-valence reaction intermediate is formed at the di-iron cofactor sites of ribonucleotide reductase and oxygenases, the unstable peroxo di-iron(III) complex formed in ferritin rapidly decays to an oxo di-iron(III) species with the concomitant release of hydrogen peroxide. The di-iron(III) oxo complex ultimately leaves the ferroxidase center of ferritins to form the iron core. Recent studies with the hyperthermophilic archaeon *P. furiosus* (Pfftn) and two ferritins from the *E. coli* bacterium (EcFtnA and EcBFR) suggested that the FC of these proteins behave similarly to the di-iron cofactor enzymes in that the di-iron complex at the FC acts as a stable cofactor during the course of iron oxidative deposition rather than a catalytic center for iron oxidation and removal [47,54,79,80] (Bou-Abdallah et al., unpublished results). These results combined with the similarities of the di-iron site ligands and the DNA codons suggest that ferritin and the di-iron cofactor enzymes may have originated from a common ancestor. It would be of interest to examine whether a stable di-iron ferroxidase complex might also form at the FC of other ferritins and is not just a characteristic of Pfftn, EcBFR, and EcFtnA. Future experiments will need to be devised to help answer this question and better define and understand the reason(s) for the

different reaction pathways and iron-protein intermediates during iron oxidation and deposition in ferritins and other di-iron proteins.

Acknowledgements

This work was supported by a Research Corporation grant (Cottrell College Science Award No. 7892) and by the Faculty Undergraduate Summer Research Program (FUSRP 2009) from SUNY Potsdam.

References

- [1] S.C. Andrews, Iron storage in bacteria, *Adv. Microbiol. Physiol.* 40 (1998) 281–351.
- [2] M. Miethke, M. Marahiel, Siderophore-based iron acquisition and pathogen control, *Microbiol. Mol. Biol. Rev.* 71 (2007) 413–451.
- [3] J.B. Neilands, Siderophores: structure and function of microbial iron transport compounds, *J. Biol. Chem.* 270 (1995) 26723–26726.
- [4] J.-F. Briat, cellular and whole organism aspects of iron transport and storage in plants, in: M.J. Tamás, E. Martinoia (Eds.), *Molecular Biology of Metal Homeostasis and Detoxification*, Topics in Current Genetics, vol. 14, Springer-Verlag, Berlin Heidelberg, 2005, pp. 193–213.
- [5] R.R. Crichton, R.J. Ward, An overview of iron metabolism: molecular and cellular criteria for the selection of iron chelators, *Curr. Med. Chem.* 10 (2003) 997–1004.
- [6] S.C. Andrews, A.K. Robinson, F. Rodriguez-Quinones, Bacterial iron homeostasis, *FEMS Microbiol. Rev.* 27 (2003) 215–237.
- [7] P. Wardman, L.P. Candeias, Fenton chemistry: an introduction, *Rad. Res.* 145 (1996) 523–531.
- [8] P.M. Harrison, P. Arosio, The ferritins: molecular properties, iron storage function and cellular regulation, *Biochim. Biophys. Acta* 1275 (1996) 161–203.
- [9] N.D. Chasteen, Ferritin. Uptake, storage, and release of iron, *Met. Ions Biol. Syst.* 35 (1998) 479–514.
- [10] P. Arosio, R. Ingrassia, P. Cavadini, Ferritins: a family of molecules for iron storage, antioxidation and more, *Biochim. Biophys. Acta* 1790 (7) (2009) 589–599.
- [11] E.C. Theil, The ferritin family of iron storage proteins, *Adv. Enzymol. Relat. Areas Mol. Biol.* 63 (1990) 421–449.
- [12] F. Missirlis, S. Kosmidis, T. Brody, M. Mavrikis, S. Holmberg, W.F. Odenwald, E.M. Skoulakis, T.A. Rouault, Homeostatic mechanisms for iron storage revealed by genetic manipulations and live imaging of *Drosophila* ferritin, *Genetics* 177 (2007) 89–100.
- [13] C. Ferreira, D. Bucchini, M.E. Martin, S. Levi, P. Arosio, B. Grandchamp, C. Beaumont, Early embryonic lethality of H ferritin gene deletion in mice, *J. Biol. Chem.* 275 (2000) 3021–3024.
- [14] K. Thompson, S. Menzies, M. Muckenthaler, F.M. Torti, T. Wood, S.V. Torti, M.W. Hentze, J. Beard, J. Connor, Mouse brains deficient in H-ferritin have normal iron concentration but a protein profile of iron deficiency and increased evidence of oxidative stress, *J. Neurosci. Res.* 71 (2003) 46–63.
- [15] A. Kauko, S. Haataja, A.T. Pulliainen, J. Finne, A.C. Papageorgiou, Crystal structure of *Streptococcus suis* Dps-like peroxide resistance protein Dpr: implications for iron incorporation, *J. Mol. Biol.* 338 (2004) 547–558.
- [16] E.R. Rocha, J.G. Owens, C.J. Smith, The redox-sensitive transcriptional activator oxyR regulates the peroxide response regulon in the obligate anaerobe *Bacteroides fragilis*, *J. Bacteriol.* 182 (2000) 5059–5069.
- [17] E.C. Theil, M. Matzapetakis, X. Liu, Ferritins: iron/oxygen biominerals in protein nanocages, *J. Biol. Inorg. Chem.* 11 (2006) 803–810.
- [18] A.C. Lewin, G.R. Moore, N.E. Le Brun, Formation of protein-coated iron minerals, *Dalton Trans.* 21 (2005) 3597–3610.
- [19] E. Chiancone, P. Ceci, A. Ilari, F. Ribacchi, S. Stefanini, Iron and proteins for iron storage and detoxification, *Biometals* 17 (2004) 197–202.
- [20] G. Zhao, P. Arosio, N.D. Chasteen, Iron(II) and hydrogen peroxide detoxification by human H-chain ferritin. An EPR spin-trapping study, *Biochemistry* 45 (2006) 3429–3436.
- [21] K.J. Thompson, M.G. Fried, Z. Ye, P. Boyer, J.R. Connor, Regulation, mechanisms and proposed function of ferritin translocation to cell nuclei, *J. Cell Sci.* 115 (2002) 2165–2177.
- [22] X. Liu, E. Theil, Ferritins: dynamic management of biological iron and oxygen chemistry, *Acc. Chem. Res.* 38 (2005) 167–175.
- [23] F. Bou-Abdallah, G. Biasiotto, P. Arosio, N.D. Chasteen, The putative nucleation site in human H-chain ferritin is not required for mineralization of the iron core, *Biochemistry* 43 (2004) 4332–4337.
- [24] M.E.M. Rocha, F. Dutra, B. Bandy, R.L. Baldini, S.L. Gomes, A. Faljoni-Alario, C.W. Liria, M.T.M. Miranda, E.J.H. Bechara, Oxidative damage to ferritin by 5-aminolevulinic acid, *Arch. Biochem. Biophys.* 409 (2003) 349–356.
- [25] R. Scudiero, F. Trinchella, E. Parisi, Iron metabolism genes in antarctic notothenioids: a review, *Mar. Genomics* 1 (2008) 79–85.
- [26] F. Bou-Abdallah, P. Santambrogio, S. Levi, P. Arosio, N.D. Chasteen, Unique iron binding and oxidation properties of human mitochondrial ferritin: a comparative analysis with human H-chain ferritin, *J. Mol. Biol.* 347 (2005) 543–554.
- [27] A.S. Pereira, W. Small, C. Krebs, P. Tavares, D.E. Edmondson, E.C. Theil, B.H. Huynh, Direct spectroscopic and kinetic evidence for the involvement of a peroxidoferric intermediate during the ferroxidase reaction in fast ferritin mineralization, *Biochemistry* 37 (1998) 9871–9876.
- [28] N.E. Le Brun, A.J. Thomson, G.R. Moore, Metal centres of bacterioferritin or non-haem iron containing cytochromes *b₅₅₇*, *Struct. Bonding* 88 (1997) 103–138.
- [29] X. Yang, N.E. Le Brun, A.J. Thomson, G.R. Moore, N.D. Chasteen, The iron oxidation and hydrolysis chemistry of *Escherichia coli* bacterioferritin, *Biochemistry* 39 (2000) 4915–4923.
- [30] A. Ilari, S. Stefanini, E. Chiancone, D. Tsernoglou, The dodecameric ferritin from *Listeria innocua* contains a novel intersubunit iron-binding site, *Nat. Struct. Biol.* 7 (2000) 38–43.
- [31] F. Bou-Abdallah, P. Arosio, S. Levi, C. Janus-Chandler, N.D. Chasteen, Defining metal ion inhibitor interactions with recombinant human H- and L-chain ferritins and site-directed variants: an isothermal titration calorimetry study, *J. Biol. Inorg. Chem.* 8 (2003) 489–497.
- [32] F. Bou-Abdallah, P. Arosio, P. Santambrogio, X. Yang, C. Janus-Chandler, N.D. Chasteen, Ferrous ion binding to recombinant human H-chain ferritin. An isothermal titration calorimetry study, *Biochemistry* 41 (2002) 11184–11191.
- [33] E.C. Theil, H. Takagi, G.W. Small, L. He, A.R. Tipton, D. Danger, The ferritin iron entry and exit problem, *Inorg. Chim. Acta* 297 (2000) 242–251.
- [34] S. Levi, P. Santambrogio, B. Corsi, A. Cozzi, P. Arosio, Evidence that residues exposed on the three-fold channels have active roles in the mechanism of ferritin iron incorporation, *Biochem. J.* 317 (1996) 467–473.
- [35] F. Bou-Abdallah, G. Zhao, G. Biasiotto, M. Poli, P. Arosio, N.D. Chasteen, Facilitated diffusion of iron(II) and dioxygen substrates into human H-chain ferritin, a fluorescence and absorbance study employing the ferroxidase center substitution, Y34W, *J. Am. Chem. Soc.* 130 (52) (2008) 17801–17811.
- [36] T. Douglas, D.R. Ripoli, Calculated electrostatic gradients in recombinant human H-chain ferritin, *Protein Sci.* 7 (1998) 1083–1109.
- [37] G.D. Watt, D. Jacobs, R.B. Frankel, Redox reactivity of bacterial and mammalian ferritin: is reductant entry into the ferritin interior a necessary step for iron release? *Proc. Natl. Acad. Sci. USA* 85 (1988) 7457–7461.
- [38] X. Yang, N.D. Chasteen, Molecular diffusion into horse spleen ferritin: a nitroxide radical spin probe study, *Biophys. J.* 71 (1996) 1587–1595.
- [39] X. Yang, P. Arosio, N.D. Chasteen, Molecular diffusion into ferritin. Pathways, temperature dependence, incubation time and concentration effects, *Biophys. J.* 78 (2000) 2049–2059.
- [40] N.D. Chasteen, P.M. Harrison, Mineralization in ferritin: an efficient means of iron storage, *J. Struct. Biol.* 126 (1999) 182–194.
- [41] X.S. Liu, L.D. Patterson, M.J. Miller, E.C. Theil, Peptides selected for the protein nanocage pores change the rate of iron recovery from the ferritin mineral, *J. Biol. Chem.* 282 (2007) 31821–31825.
- [42] W. Jin, H. Takagi, B. Pancorbo, E.C. Theil, Opening the ferritin pore for iron release by mutation of conserved amino acids at interhelix and loop sites, *Biochemistry* 40 (2001) 7525–7532.
- [43] A. Dautant, J.B. Meyer, J. Yariv, G. Precigoux, R.M. Sweet, A.J. Kalb, F. Frolow, Structure of a monoclinic crystal form of cytochrome *b₁* (bacterioferritin) from *E. coli*, *Acta Crystallogr. D* 54 (1998) 16–24.
- [44] T.J. Stillman, P.D. Hempstead, P.J. Artymiuik, S.C. Andrews, A.J. Hudson, A. Treffry, J. R. Guest, P.M. Harrison, The high-resolution X-ray crystallographic structure of the ferritin (EcFtnA) of *Escherichia coli*; comparison with human H ferritin (HuHF) and the structures of the Fe³⁺ and Zn²⁺ derivatives, *J. Mol. Biol.* 307 (2001) 587–603.
- [45] H.-L. Liu, H.-N. Zhou, W.-M. Xing, J.-F. Zhao, S.-X. Li, J.-F. Huang, R.-C. Bi, 2.6 Å resolution crystal structure of the bacterioferritin from *Azotobacter vinelandii*, *FEBS Lett.* 573 (2004) 93–98.
- [46] L. Swartz, M. Kuchinskas, H. Li, T.L. Poulos, W.N. Lanzilotta, Redox-dependent structural changes in the *azotobacter vinelandii* bacterioferritin: new insights into the ferroxidase and iron transport mechanism, *Biochemistry* 45 (2006) 4421–4428.
- [47] J. Tatur, W.R. Hagen, P.M. Matias, Crystal structure of the ferritin from the hyperthermophilic archaeal anaerobe *Pyrococcus furiosus*, *J. Biol. Inorg. Chem.* 12 (2007) 615–630.
- [48] E. Johnson, D. Cascio, M.R. Sawaya, M. Gingery, I. Schröder, Crystal structures of a tetrahedral open pore ferritin from the hyperthermophilic archaeon *Archaeoglobus fulgidus*, *Structure* 13 (2005) 637–648.
- [49] S. Macedo, C.V. Romao, E. Mitchell, P.M. Matias, M.Y. Liu, A.V. Xavier, J. LeGall, M. Teixeira, P. Lindley, M.A. Carrondo, The nature of the di-iron site in the bacterioferritin from *Desulfovibrio desulfuricans*, *Nat. Struct. Biol.* 10 (2003) 285–290.
- [50] M.A. Carrondo, Ferritins, iron uptake and storage from the bacterioferritin viewpoint, *EMBO J.* 22 (2003) 1959–1968.
- [51] P. Santambrogio, S. Levi, A. Cozzi, E. Rovida, A. Albertini, P. Arosio, Production and characterization of recombinant heteropolymers of human ferritin H and L chains, *J. Biol. Chem.* 268 (1993) 12744–12748.
- [52] S. Sun, P. Arosio, S. Levi, N.D. Chasteen, Ferroxidase kinetics of human liver apoferritin, recombinant H-chain apoferritin, and site-directed mutants, *Biochemistry* 32 (1993) 9362–9369.
- [53] G. Zhao, F. Bou-Abdallah, P. Arosio, S. Levi, C. Janus-Chandler, N.D. Chasteen, Multiple pathways for mineral core formation in mammalian apoferritin. The role of hydrogen peroxide, *Biochemistry* 42 (2003) 3142–3150.
- [54] K.H. Ebrahimi, P.-L. Hagedoorn, J.A. Jongejans, W.R. Hagen, Catalysis of iron core formation in *Pyrococcus furiosus* ferritin, *J. Biol. Inorg. Chem.* 14 (2009) 1265–1274.
- [55] A. Treffry, Z. Zhao, M.A. Quail, J.R. Guest, P.M. Harrison, Dinuclear center of ferritin: studies of iron binding and oxidation show differences in the two iron sites, *Biochemistry* 36 (1997) 432–441.
- [56] G. Zhao, F. Bou-Abdallah, X. Yang, P. Arosio, N.D. Chasteen, Is hydrogen peroxide produced during iron(II) oxidation in mammalian apoferritins? *Biochemistry* 40 (2001) 10832–10838.

- [57] F. Bou-Abdallah, G. Papaefthymiou, D.S. Scheswohl, S. Stanga, P. Arosio, N.D. Chasteen, μ -1, 2-Peroxo-bridged di-iron(III) dimer formation in human H-chain ferritin, *Biochem. J.* 364 (2002) 57–63.
- [58] G. Zhao, M. Su, N.D. Chasteen, μ -1, 2-Peroxo diferric complex formation in horse spleen ferritin. A mixed H/L-subunit heteropolymer, *J. Mol. Biol.* 352 (2005) 467–477.
- [59] P. Moenne-Loccoz, C. Krebs, K. Herlihy, D.E. Edmondson, E.C. Theil, B.H. Huynh, T. M. Loehr, The ferroxidase reaction of ferritin reveals a diferric μ -1, 2 bridging peroxide intermediate in common with other O_2 -activating non-heme di-iron proteins, *Biochemistry* 38 (1999) 5290–5295.
- [60] A. Treffry, Z. Zhao, M.A. Quail, J.R. Guest, P.M. Harrison, How the presence of three iron binding sites affects the iron storage function of the ferritin (EcFtnA) of *Escherichia coli*, *FEBS Lett.* 432 (1998) 213–218.
- [61] F. Bou-Abdallah, A.C. Lewin, N.E. Le Brun, G.R. Moore, N.D. Chasteen, Iron detoxification properties of *Escherichia coli* bacterioferritin attenuation of oxyradical chemistry, *J. Biol. Chem.* 277 (2002) 37064–37069.
- [62] F. Bou-Abdallah, G. Zhao, H.R. Mayne, P. Arosio, N.D. Chasteen, Origin of the unusual kinetics of iron deposition in human H-chain ferritin, *J. Am. Chem. Soc.* 127 (2005) 3885–3893.
- [63] G.N.L. Jameson, W. Jin, C. Krebs, A.S. Pereira, P. Tavares, X. Liu, E.C. Theil, B.H. Huynh, Stoichiometric production of hydrogen peroxide and parallel formation of ferric multimers through decay of the diferric-peroxo complex, the first detectable intermediate in ferritin mineralization, *Biochemistry* 41 (2002) 13435–13443.
- [64] H. Aitken-Rogers, C. Singleton, A. Lewin, A. Taylor-Gee, G.R. Moore, N.E. Le Brun, Effect of phosphate on bacterioferritin-catalysed iron(II) oxidation, *J. Biol. Inorg. Chem.* 9 (2004) 161–170.
- [65] R.R. Crichton, F. Roman, A novel mechanism for ferritin iron oxidation and deposition, *J. Mol. Catal.* 4 (1978) 75.
- [66] I.G. Macara, T.G. Hoy, P.M. Harrison, The formation of ferritin from apoferritin. Kinetics and mechanism of iron uptake, *Biochem. J.* 126 (1972) 151.
- [67] S. Lindsay, D. Brosnahan, T.J. Lowery Jr., K. Crawford, G.D. Watt, Kinetic studies of iron deposition in horse spleen ferritin using O_2 as oxidant, *Biochim. Biophys. Acta* 1621 (2003) 57–66.
- [68] T.J. Lowery, J. Bunker, B. Zhang, R. Costen, G.D. Watt, Kinetic studies of iron deposition in horse spleen ferritin using O_2 and H_2O_2 as oxidant, *Biophys. Chem.* 111 (2004) 173–181.
- [69] P.M. Proulx-Curry, N.D. Chasteen, Molecular aspects of iron uptake and storage in ferritin, *Coord. Chem. Rev.* 144 (1995) 347–368.
- [70] X. Liu, E. Theil, Ferritin reactions: direct identification of the site for the diferric peroxide reaction intermediate, *PNAS* 101 (23) (2004) 8557–8562.
- [71] S. Sun, P. Arosio, S. Levi, N.D. Chasteen, Ferroxidase kinetics of human liver apoferritin, recombinant H-chain apoferritin, and site-directed mutants, *Biochemistry* 32 (1993) 9362–9369.
- [72] V.J. Wade, S. Levi, P. Arosio, A. Treffry, P.M. Harrison, S. Mann, Influence of site-directed modifications on the formation of iron cores in ferritin, *J. Mol. Biol.* 221 (1991) 1443–1452.
- [73] E.R. Bauminger, P.M. Harrison, D. Hechel, I. Nowik, A. Treffry, Mössbauer spectroscopic investigation of structure function relations in ferritins, *Biochim. Biophys. Acta* 1118 (1991) 48–58.
- [74] J. Hwang, C. Krebs, B.H. Huynh, D.E. Edmondson, E.C. Theil, J.E. Penner-Hahn, A short Fe–Fe distance in peroxodiferric ferritin: control of Fe substrate versus cofactor decay? *Science* 287 (2000) 122–125.
- [75] P.M. Harrison, P.D. Hempstead, P.J. Artymiuk, S.C. Andrews, Structure–function relationships in the ferritins, in: H. Sigel, A. Sigel (Eds.), *Met. Ions. Biol. Syst.*, vol. 35, Dekker, New York, 1998, pp. 435–477.
- [76] L. Smith, The physiological role of ferritin-like compounds in bacteria, *Crit. Rev. Microbiol.* 30 (2004) 173–185.
- [77] A. Treffry, Z. Zhao, M.A. Quail, J.R. Guest, P.M. Harrison, The use of zinc(II) to probe iron binding and oxidation by the ferritin (EcFtnA) of *Escherichia coli*, *J. Biol. Inorg. Chem.* 3 (1998) 682–688.
- [78] S. Baaghil, A. Lewin, G.R. Moore, N.E. Le Brun, Core formation in *Escherichia coli* bacterioferritin requires a functional ferroxidase center, *Biochemistry* 42 (2003) 14047–14056.
- [79] A. Crow, T.L. Lawson, A. Lewin, G.R. Moore, N.E. Le Brun, Structural basis for iron mineralization by bacterioferritin, *J. Am. Chem. Soc.* 131 (2009) 6808–6813.
- [80] T.L. Lawson, L. Crow, A. Lewin, S. Yasmin, G.R. Moore, N.E. Le Brun, Monitoring the iron status of the ferroxidase center of *Escherichia coli* bacterioferritin using fluorescence spectroscopy, *Biochemistry* 48 (2009) 9031–9039.
- [81] F. Bou-Abdallah, M.R. Woodhall, A. Velásquez-Campoy, S.C. Andrews, N.D. Chasteen, Thermodynamic analysis of ferrous ion binding to *Escherichia coli* ferritin EcFtnA, *Biochemistry* 44 (2005) 13837–13846.
- [82] J. Bunker, T. Lowery, G. Davis, B. Zhang, D. Brosnahan, S. Lindsay, R. Costen, S. Choi, P. Arosio, G.D. Watt, Kinetic studies of iron deposition catalyzed by recombinant human liver heavy, and light ferritins and *Azotobacter vinelandii* bacterioferritin using O_2 and H_2O_2 as oxidants, *Biophys. Chem.* 114 (2005) 235–244.
- [83] B. Zhang, G.D. Watt, Anaerobic iron deposition into horse spleen, recombinant human heavy and light and bacteria ferritins by large oxidants, *J. Inorg. Biochem.* 101 (2007) 1676–1685.
- [84] E.C. Theil, D.J. Goss, Living with iron (and oxygen): questions and answers about iron homeostasis, *Chem. Rev.* 109 (10) (2009) 4568–4579.
- [85] B. Wiedenheft, J. Mosolf, D. Willits, M. Yeager, K.A. Dryden, M. Young, T. Douglas, An archaeal antioxidant: characterization of a Dps-like protein from *Sulfolobus solfataricus*, *Proc. Natl. Acad. Sci. U.S.A.* 102 (30) (2005) 10551–10556.
- [86] J.K. Schwartz, X.S. Liu, T. Toshi, E.C. Theil, E.L. Solomon, Spectroscopic definition of the ferroxidase site in M ferritin: comparison of binuclear substrate vs. cofactor active sites, *J. Am. Chem. Soc.* 130 (2008) 9441–9450.
- [87] T. Toshi, M.R. Hasan, E.C. Theil, The ferritin Fe2 site at the di-iron catalytic center controls the reaction with O_2 in the rapid mineralization pathway, *PNAS* 105 (47) (2008) 18182–18187.
- [88] C.V. Romao, R. Louro, R. Timkovich, M. Lubben, M.Y. Liu, J. LeGall, A.V. Xavier, M. Teixeira, Iron-coproporphyrin III is a natural cofactor in bacterioferritin from the anaerobic bacterium *Desulfovibrio desulfuricans*, *FEBS Lett.* 480 (2000) 213–216.
- [89] L. Toussaint, L. Bertrand, L. Hue, R.R. Crichton, J.P. Declercq, High-resolution X-ray structures of human apoferritin H-chain mutants correlated with their activity and metal-binding sites, *J. Mol. Biol.* 365 (2007) 440–452.
- [90] P. Turano, D. Lalli, I.C. Felli, E.C. Theil, I. Bertini, NMR reveals pathway for ferric mineral precursors to the central cavity of ferritin, *PNAS* 107 (2) (2010) 545–550.
- [91] B. Langlois d'Estaintot, P. Santambrogio, T. Granier, B. Gallois, J.M. Chevalier, G. Precigoux, S. Levi, P. Arosio, Crystal structure and biochemical properties of the human mitochondrial ferritin and its mutant Ser144Ala, *J. Mol. Biol.* 340 (2004) 277–293.
- [92] P.D. Hempstead, S.J. Yewdall, A.R. Fernie, D.M. Lawson, P.J. Artymiuk, D.W. Rice, G. C. Ford, P.M. Harrison, Comparison of the three-dimensional structures of recombinant human H and horse L ferritins at high resolution, *J. Mol. Biol.* 268 (1997) 424–448.
- [93] S.C. Willies, M.N. Isupov, E.F. Garman, J.A. Littlechild, The binding of haem and zinc in the 1.9 Å X-ray structure of *Escherichia coli* bacterioferritin, *J. Biol. Inorg. Chem.* 14 (2009) 201–207.
- [94] T.J. Stillman, P.P. Connolly, C.L. Latimer, A.F. Morland, M.A. Quail, S.C. Andrews, A. Treffry, J.R. Guest, P.J. Artymiuk, P.M. Harrison, Insights into the effects on metal binding of the systematic substitution of five key glutamate ligands in the ferritin of *Escherichia coli*, *J. Biol. Chem.* 278 (28) (2003) 26275–26286.
- [95] S. Macedo, C.V. Romao, E. Mitchell, P.M. Matias, M.Y. Liu, A.V. Xavier, J. LeGall, M. Teixeira, P. Lindley, M.A. Carrondo, The nature of the di-iron site in the bacterioferritin from *Desulfovibrio desulfuricans*, *Nat. Struct. Biol.* 10 (2003) 285–290.
- [96] X. Yang, Y. Chen-Barrett, P. Arosio, N.D. Chasteen, Reaction paths of iron oxidation and hydrolysis in horse spleen and recombinant human ferritins, *Biochemistry* 37 (27) (1998) 9743–9750.
- [97] B. Xu, N.D. Chasteen, Iron oxidation chemistry in ferritin. Increasing Fe/ O_2 stoichiometry during core formation, *J. Biol. Chem.* 266 (1991) 19965–19970.